Placental growth factor stabilizes VEGF receptor-2 protein in retinal pigment epithelial cells by downregulating glycogen synthase kinase 3 activity

Miyuki Murata[1,2], Kousuke Noda[1,2,*], Satoru Kase[1,2], Keitaro Hase[1,2], Di Wu[1,2], Ryo Ando[2], and Susumu Ishida[1,2]

From the [1]Laboratory of Ocular Cell Biology & Visual Science, and [2]Department of Ophthalmology, Faculty of Medicine and Graduate School of Medicine, Hokkaido University, Sapporo, Japan

Edited by Henrik Dohlman

Placental growth factor (PlGF) belongs to the vascular endothelial growth factor (VEGF) family of proteins that participate in angiogenesis and vasculogenesis. Anti-VEGF therapy has become the standard treatment for ocular angiogenic disorders in ophthalmological practice. However, there is emerging evidence that anti-VEGF treatment may increase the risk of atrophy of the retinal pigment epithelium (RPE), which is important for the homeostasis of retinal tissue. Whereas the cytoprotective role of VEGF family molecules, particularly that of VEGF A (VEGFA) through its receptor VEGF receptor-2 (VEGFR-2), has been recognized, the physiological role of PlGF in the retina is still unknown. In this study, we explored the role of PlGF in the RPE using PlGF-knockdown RPE cells generated by retrovirus-based PlGF-shRNA transduction. We show that VEGFA reduced apoptosis induced by serum starvation in RPE cells, whereas the antiapoptotic effect of VEGFA was abrogated by VEGFR-2 knockdown. Furthermore, PlGF knockdown increased serum starvation–induced cell apoptosis and unexpectedly reduced the protein level of VEGFR-2 in the RPE. The antiapoptotic effect of VEGFA was also diminished in PlGF-knockdown RPE cells. In addition, we found that glycogen synthase kinase 3 activity was involved in proteasomal degradation of VEGFR-2 in RPE cells and inactivated by PlGF via AKT phosphorylation. Overall, the present data demonstrate that PlGF is crucial for RPE cell viability and that PlGF supports VEGFA/VEGFR-2 signaling by stabilizing the VEGFR-2 protein levels through glycogen synthase kinase 3 inactivation.

Placental growth factor (PlGF) is a secreted dimeric glycoprotein belonging to the vascular endothelial growth factor (VEGF) family (1). Similar to other VEGF family ligands, PlGF participates in eliciting pathological changes in blood vessels, such as pathological angiogenesis (2) and vascular leakage (3), and thus plays a role in the pathogenesis of a variety of angiogenic disorders. Four isoforms of PlGF generated through alternative mRNA splicing have been identified to date (4); of these, PlGF-1 and PlGF-2 are considered to be the dominant isoforms. PlGF-1 binds to VEGF receptor-1 (VEGFR-1), whereas PlGF-2 binds to neuropilin-1 (NRP1) and neuropilin-2 (NRP2) in endothelial cells and other cell types, such as neuronal cells (5). Previous studies revealed that PlGF transduces its signaling by binding to VEGFR-1 and amplifies VEGF A (VEGFA)-driven angiogenesis via multiple mechanisms, including (1) promotion of VEGF binding to VEGFR-2 and (2) regulation of crosstalk between VEGFR-1 and VEGFR-2 (6). However, the detailed mechanism, which enhances VEGFA/VEGFR signaling in the presence of PlGF, remains elusive.

In the field of ophthalmology, intravitreal injection of anti-VEGF agents is now widely used in the treatment of ocular angiogenic disorders, including neovascular age-related macular degeneration (AMD). Anti-VEGF therapy has become the standard treatment for neovascular AMD and has improved the visual prognosis of patients with central visual disturbance. However, there is emerging evidence that anti-VEGF treatment may potentially expose the macula to the risk of atrophy of the retinal pigment epithelium (RPE) (7–11), a monolayer of pigmented cells between the neuroretina and the choroid. All anti-VEGF agents currently used in clinical practice target VEGFA as a basic strategy to inhibit ocular angiogenesis. However, in vitro experiments in previous studies have demonstrated that VEGFA neutralization causes apoptosis (8) and leads to cellular vulnerability to oxidative stress (7) in RPE cells. In addition, a multicenter cohort study that surveyed the long-term effects of anti-VEGF treatment in patients with neovascular AMD revealed that macular atrophy was present in 98% of the study eyes at a mean of 7.3 years after anti-VEGF treatment (11). Furthermore, other clinical studies have also demonstrated an increase in the incidence of macular atrophy after anti-VEGF treatment for neovascular AMD (9, 10). Therefore, several lines of evidence indicate that long-term VEGFA blockade may cause RPE atrophy. In contrast, the influence of PlGF blockade on the RPE remains to be elucidated, although PlGF is also a target molecule of one of the anti-VEGF agents currently used in clinical practice.

In the present study, we sought to explore the cytoprotective effects of PlGF in the RPE.
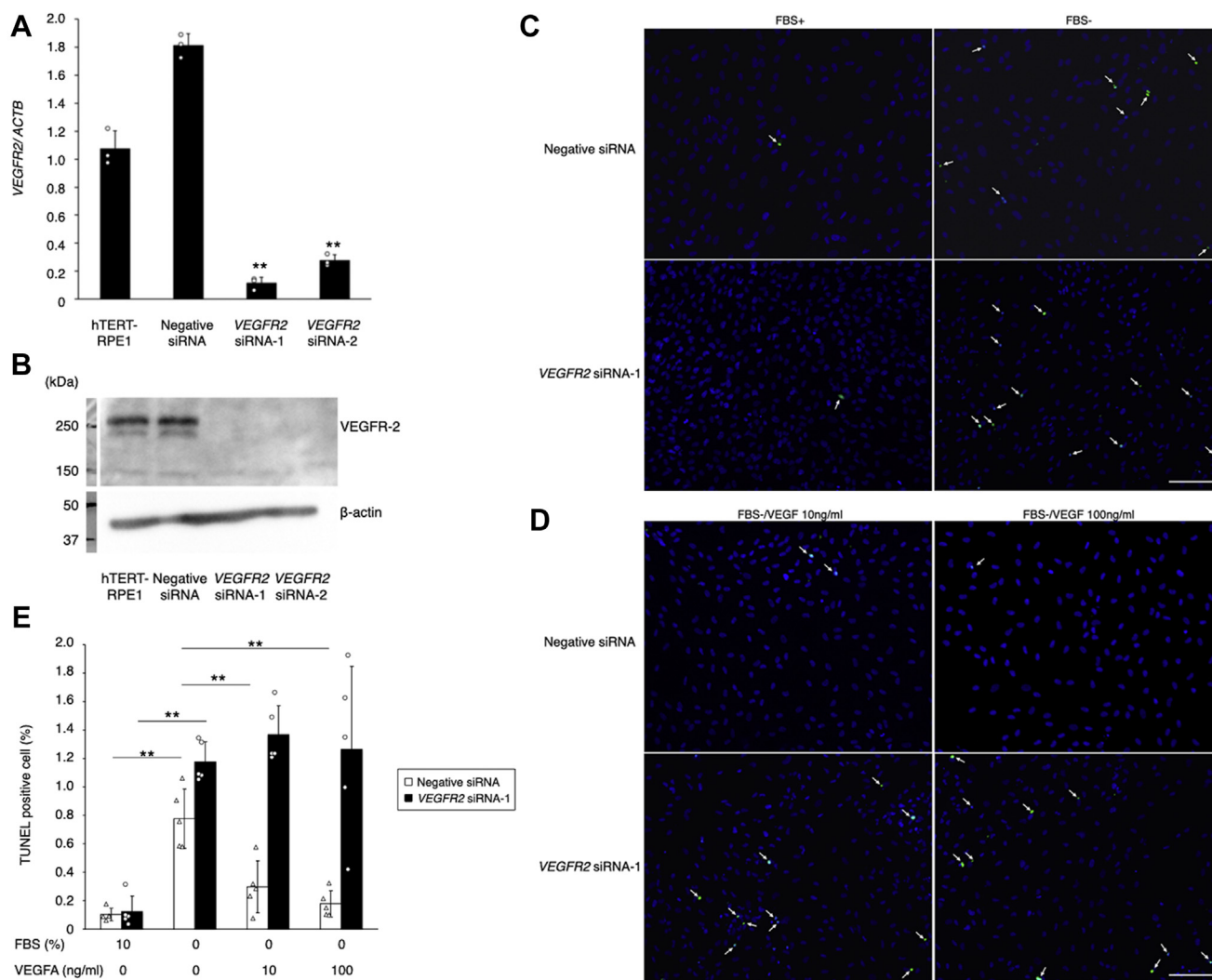
Figure 1. Effect of VEGFR-2 knockdown on the survival of hTERT-RPE1 cells under serum starvation stress. *A*, *VEGFR2* mRNA expression in hTERT-RPE1 cells transfected with *VEGFR2* siRNA (10 nM) for 48 h, analyzed by real-time PCR (n = 3 each, **$p < 0.01$). *B*, VEGFR-2 protein in hTERT-RPE1 cells transfected with *VEGFR2* siRNA (10 nM) for 72 h and analyzed by Western blotting. *C* and *D*, representative micrographs of TUNEL staining in hTERT-RPE1 cells transfected with negative control siRNA or *VEGFR2* siRNA-1. Cells were serum starved for 24 h with or without VEGFA recombinant protein (10–100 ng/ml). The scale bar represents 100 µm. *E*, TUNEL-positive cell rate of hTERT-RPE1 cells transfected with negative control siRNA or *VEGFR2* siRNA-1 (10–100 ng/ml, n = 5 each, *$p < 0.05$, **$p < 0.01$). RPE, retinal pigment epithelium; VEGFR-2, vascular endothelial growth factor receptor-2.

Results

VEGFA/VEGFR-2 cascade is required for RPE cell survival under serum starvation stress

Since the VEGFA/VEGFR-2 cascade is known to play a protective role in retinal ganglion cells in ischemia-driven neural cell death (12), we first examined the influence of VEGFR-2 knockdown in cultured human RPE cells, hTERT-RPE1. After *VEGFR2* siRNA transfection into hTERT-RPE1, the efficiency of VEGFR-2 knockdown was validated by real-time PCR (n = 3 each, $p < 0.01$, Fig. 1A) and Western blotting (Fig. 1B).

Serum starvation induced apoptosis in both negative control siRNA- and *VEGFR2* siRNA-transfected hTERT-RPE1 cells in comparison with cells that were not serum starved (n = 5, $p < 0.01$, Fig. 1, *C* and *E*). In addition, supplementation with VEGFA reduced the apoptosis induced by serum starvation in negative control siRNA-transfected hTERT-RPE1 cells in a

dose-dependent manner (n = 5, $p < 0.05$, Fig. 1, *D* and *E*), whereas the antiapoptotic effect of VEGFA was abrogated in VEGFR-2-knockdown hTERT-RPE1 cells (n = 5 each, Fig. 1, *D* and *E*), indicating that VEGFR-2 mediates the protective effect of VEGFA in RPE cells under serum starvation stress.

PlGF knockdown causes serum starvation–induced apoptosis in RPE cells

To investigate the effects of PlGF knockdown in human RPE cells, the cell-proliferation rate and apoptosis were investigated in hTERT-RPE1 cells after transduction with retrovirus-based PlGF shRNA. The efficiency of PlGF knockdown was validated by real-time PCR (n = 3 each, $p < 0.01$, Fig. 2A), Western blotting (Fig. 2B), and ELISA (n = 3 each, $p < 0.01$, Fig. 2C). Of the four splice variants of PlGF, PlGF-1 and PlGF-2 were expressed in hTERT-RPE1, and both isoforms were suppressed in PlGF-knockdown hTERT-RPE1 (Fig. 2D). The cell-
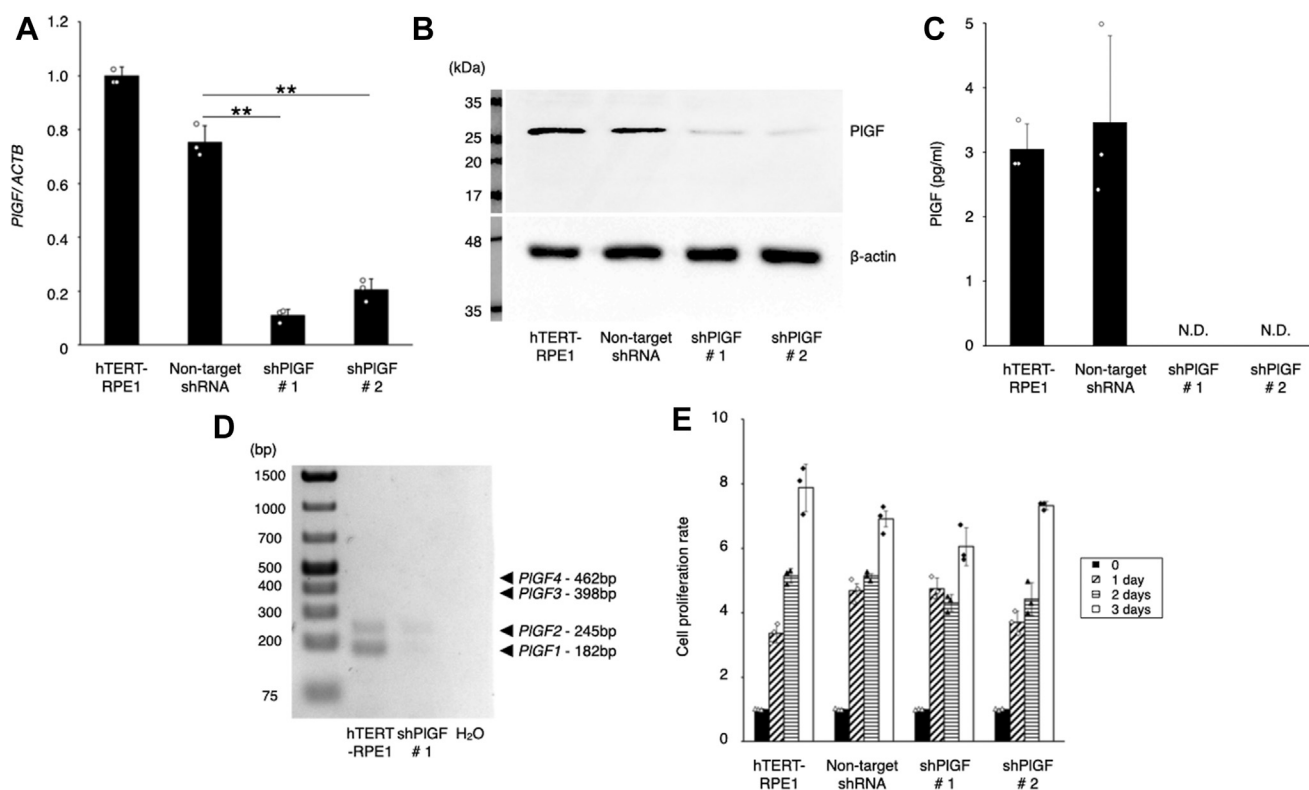
Figure 2. Cell-proliferation rate of PlGF-knockdown hTERT-RPE1. *A*, *PlGF* mRNA expression in hTERT-RPE1 cells, into which retrovirus-based *PlGF* shRNAs were transduced, analyzed by real-time PCR (n = 3 each, $**p < 0.01$). *B*, immunoblot for PlGF protein in hTERT-RPE1, nontarget shRNA, and PlGF-knockdown hTERT-RPE1 clones. *C*, PlGF protein in the supernatant of hTERT-RPE1 cells, into which retrovirus-based *PlGF* shRNAs were transduced, analyzed by ELISA (n = 3 each, ND = not detected). *D*, *PlGF* splice variants expressed in hTERT-RPE1 and PlGF-knockdown hTERT-RPE1. *E*, cell-proliferation rate of parental hTERT-RPE1, nontarget shRNA-transduced hTERT-RPE1 (nontarget shRNA), and PlGF-knockdown hTERT-RPE1 clones (n = 3 each). PlGF, placental growth factor; RPE, retinal pigment epithelium.

proliferation rate did not differ among parental hTERT-RPE1, nontarget shRNA-transfected hTERT-RPE1, and PlGF-knockdown hTERT-RPE1 cells (n = 3 each; Fig. 2E). In contrast, PlGF knockdown significantly aggravated the apoptosis induced by serum starvation in hTERT-RPE1 cells, in comparison with the apoptosis rates in both parental hTERT-RPE1 and nontarget shRNA-transfected hTERT-RPE1 cells (n = 3 each, $p < 0.01$, Fig. 3, A−C). Furthermore, activation of caspase-3/7, known to implement the cell death program, was also increased in PlGF-knockdown hTERT-RPE1 cells (n = 3 each, $p < 0.01$, Fig. 3D), in comparison with the other controls. Consistent with these data, the apoptosis caused by serum starvation in PlGF-knockdown hTERT-RPE1 cells was repressed by supplementation with either recombinant human PlGF-1 or PlGF-2 in a dose-dependent manner (n = 3 each, $p < 0.05$, $p < 0.01$, Fig. 3, E− G). These results indicate that PlGF plays a protective role against serum starvation–induced apoptosis in RPE cells.

PlGF knockdown does not affect the expression of VEGFA and its cognate receptors, except VEGFR-2, in PlGF-knockdown RPE cells

To explore the mechanism by which PlGF knockdown triggers apoptosis in human RPE cells, we examined the transcriptional changes in VEGFA and its cognate receptors, *VEGFR-1*, *VEGFR-2*, *NRP1*, and *NRP2*. There was no difference in the expression levels of *VEGFA* (n = 3 each, Fig. 4A), *VEGFR1* (n = 3 each, Fig. 4B), or *VEGFR2* (n = 3 each, Fig. 4C) between the control cells and PlGF-knockdown hTERT-RPE1 cells. In line with the mRNA data, the protein levels of VEGFA (n = 3 each, Fig. 4D), VEGFR-1 (n = 3 each, Fig. 4, E and F), NRP1, and NRP2 (data not shown) were also not altered; however, VEGFR-2 levels substantially decreased in PlGF-knockdown hTERT-RPE1 cells in comparison with the nontarget shRNA control cells (n = 3 each, $p < 0.01$, Fig. 4, G and H), and the protein degradation speed of VEGFR-2 was relatively fast in PlGF-knockdown hTERT-RPE1 cells compared with nontarget shRNA control cells (n = 3 each, $p < 0.01$, Fig. 4, I and J). In addition, the decrease in the VEGFR-2 protein level in PlGF-knockdown hTERT-RPE1 cells was attenuated by supplementation with recombinant human PlGF-1 or PlGF-2 (10 ng/ml, n = 3 each, $p < 0.05$, Fig. 4, K and L), and it was no effect for nontarget shRNA control cells (n = 3 each, Fig. 4, M and N). Furthermore, the antiapoptotic effect of VEGFA, which was repressed in VEGFR2-knockdown hTERT-RPE1 cells (Fig. 1, C−E), was also diminished in PlGF-knockdown hTERT-RPE1 cells exposed to serum starvation (n = 3 each, $p < 0.05$, Fig. 5, A−C). These results suggest that PlGF knockdown causes instability of the VEGFR-2 protein, which leads to disruption of VEGFA/VEGFR-2 signal transduction, thereby impairing the protective property of VEGFA in RPE cells.

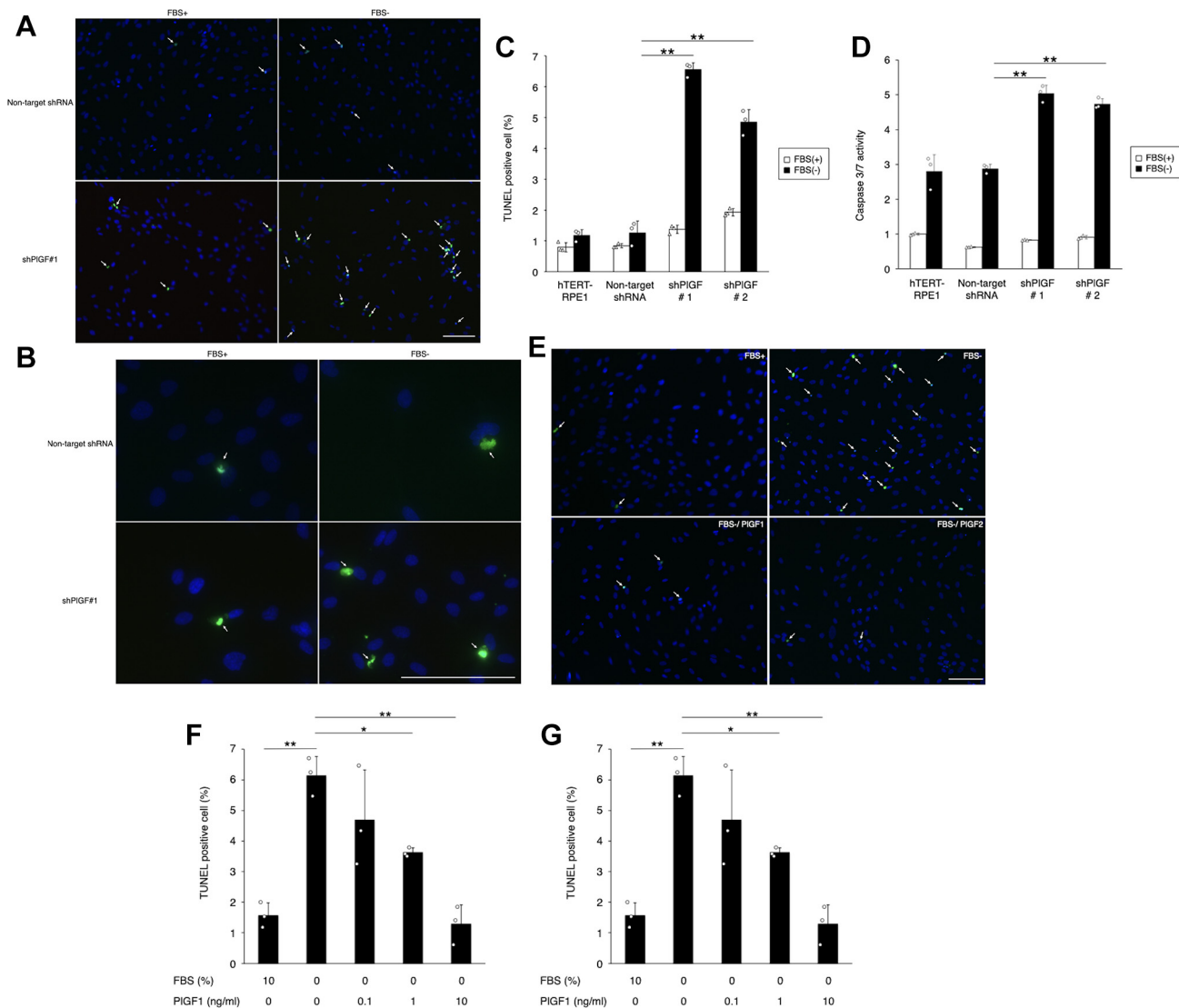SASBMB

J. Biol. Chem. (2022) 298(9) 102378 **3**

Figure 3. Impact of PlGF knockdown on cell survival of hTERT-RPE1 under serum starvation stress. *A*, representative micrographs of TUNEL staining in nontarget shRNA and PlGF-knockdown hTERT-RPE1 clones. The scale bar represents 100 μm. *B*, high-magnification images of TUNEL staining in nontarget shRNA and PlGF-knockdown hTERT-RPE1 clones. The scale bar represents 100 μm. *C*, TUNEL-positive cell rate of parental hTERT-RPE1, nontarget shRNA, and PlGF-knockdown hTERT-RPE1 clones (n = 3 each, **$p < 0.01$). Cells were serum starved for 24 h. *D*, caspase 3/7 activity in parental hTERT-RPE1, nontarget shRNA, and PlGF-knockdown hTERT-RPE1 clones (n = 3 each, **$p < 0.01$). Cells were serum starved for 24 h. *E*, representative micrographs of TUNEL staining in PlGF-knockdown hTERT-RPE1 clone #1. Cells were serum starved for 24 h with PlGF-1 or PlGF-2 recombinant protein (10 ng/ml). The scale bar represents 100 μm. *F* and *G*, TUNEL-positive cell rate of the PlGF-knockdown hTERT-RPE1 clone #1. Cells were serum starved for 24 h with PlGF-1 or PlGF-2 recombinant protein (0.1–10 ng/ml, n = 3 each, *$p < 0.05$, **$p < 0.01$). PlGF, placental growth factor; RPE, retinal pigment epithelium.

PlGF suppresses proteasomal degradation of VEGFR-2 through GSK3 inactivation

To further investigate the mechanism by which PlGF knockdown causes instability of VEGFR-2 protein, we sought to detect the molecule(s) that participate in VEGFR-2 degradation. The present study revealed that phosphorylation of GSK3α at Ser21 and GSK3β at Ser9 decreased in PlGF-knockdown hTERT-RPE1 cells in comparison with that in nontarget shRNA-transfected control cells (n = 3 each, $p < 0.01$, Fig. 6, *A* and *B*). Conversely, PlGF stimulation (10 ng/ml) enhanced the phosphorylation of GSK3α and GSK3β in PlGF-knockdown hTERT-RPE1 cells in a time-dependent manner (Fig. 6C). These data indicate that PlGF inactivates both GSK3α and GSK3β by enhancing Ser phosphorylation.

Next, to determine whether GSK3 activity is involved in VEGFR-2 degradation in RPE cells, we added a GSK3 inhibitor (CHIR99021, 0.3–3 μM) or GSK3 activator (sodium nitroprusside; 0.5–50 μM) to the PlGF-knockdown hTERT-RPE1 or parental hTERT-RPE1 cells. Strikingly, the VEGFR-2 level significantly increased when a GSK3 inhibitor was added to the PlGF-knockdown hTERT-RPE1 cells (n = 3 each, $p < 0.05$, Fig. 6, *D* and *E*), whereas the GSK3 activator remarkably decreased the VEGFR-2 level in hTERT-RPE1 cells (n = 3 each, $p < 0.05$, Fig. 6, *F* and *G*). Furthermore, the reduction in VEGFR-2 levels caused by treatment with the GSK3 activator sodium nitroprusside was recovered by treatment with the proteasome inhibitor MG132 (10 μM, n = 3 each, $p < 0.05$, Fig. 6, *H* and *I*).
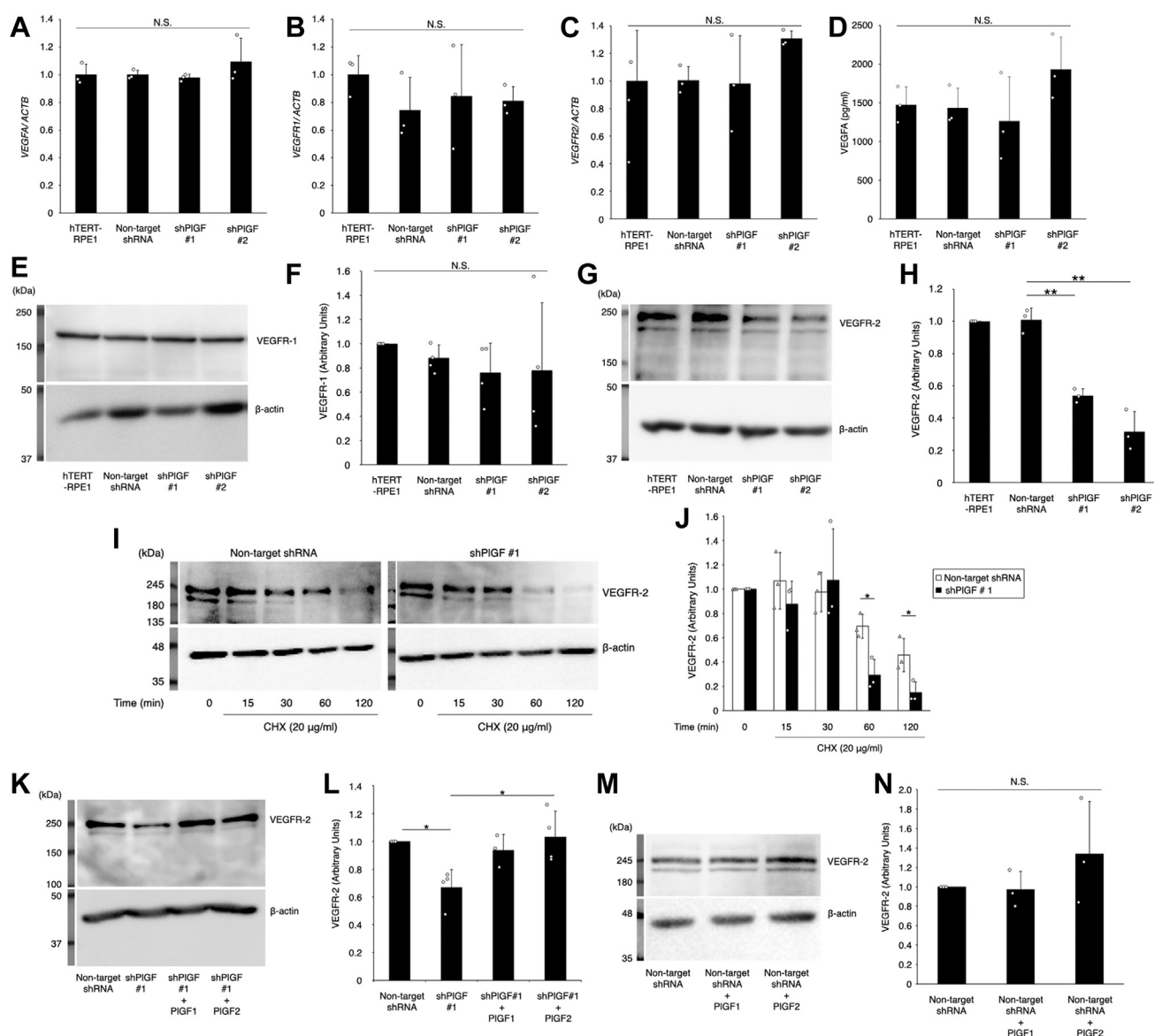
Figure 4. Expression of VEGFA and its receptors in PlGF-knockdown hTERT-RPE1. *A*, VEGFA mRNA expression in hTERT-RPE1, nontarget shRNA, and PlGF-knockdown hTERT-RPE1 clones (n = 3 each). *B*, VEGFR1 mRNA expression in hTERT-RPE1, nontarget shRNA, and PlGF-knockdown hTERT-RPE1 clones (n = 3 each). *C*, VEGFR2 mRNA expression in hTERT-RPE1, nontarget shRNA, and PlGF-knockdown hTERT-RPE1 clones (n = 3 each). *D*, VEGFA protein levels measured by ELISA in hTERT-RPE1, nontarget shRNA, and PlGF-knockdown hTERT-RPE1 clones (n = 3 each). *E* and *F*, immunoblot for VEGFR-1 protein in hTERT-RPE1, nontarget shRNA, and PlGF-knockdown hTERT-RPE1 clones (n = 4 each). *G* and *H*, immunoblot for VEGFR-2 protein in hTERT-RPE1, nontarget shRNA, and PlGF-knockdown hTERT-RPE1 clones (n = 3 each, **$p < 0.01$). *I* and *J*, immunoblot for VEGFR-2 protein in nontarget shRNA, and PlGF-knockdown hTERT-RPE1 clone #1 treated with protein synthesis inhibitor cycloheximide (CHX, 20 µg/ml) for the indicated time (n = 3 each, *$p < 0.05$). *K* and *L*, immunoblot for VEGFR-2 protein in PlGF-knockdown hTERT-RPE1 clone #1 treated with PlGF-1 or PlGF-2 recombinant protein (10 ng/ml) for 24 h (n = 4 each, *$p < 0.05$). *M* and *N*, immunoblot for VEGFR-2 protein in nontarget shRNA-hTERT-RPE1 treated with PlGF-1 or PlGF-2 recombinant protein (10 ng/ml) for 24 h (n = 3 each). PlGF, placental growth factor; RPE, retinal pigment epithelium; VEGFA, vascular endothelial growth factor A; VEGFR, VEGF receptor.

These data indicate that PlGF suppresses the proteasomal degradation of VEGFR-2 through GSK3 inactivation.

PlGF inactivates GSK3 *via* AKT phosphorylation

Finally, to elucidate the PlGF-associated molecular machinery that induces GSK3 phosphorylation, we sought to identify the signaling pathway of GSK3 phosphorylation by PlGF. The findings showed that PlGF regulates extracellular signal–regulated kinase (ERK)1/2 and AKT phosphorylation by binding to VEGFR-1 (13, 14). Consistent with previous reports, human recombinant PlGF-1 and

PlGF-2 upregulated ERK1/2 and AKT phosphorylation in PlGF-knockdown hTERT-RPE1 cells (Fig. 7*A*). Furthermore, in PlGF-knockdown hTERT-RPE1 cells, the mitogen-activated protein kinase kinase inhibitor U0126 (10 µM) suppressed ERK1/2 phosphorylation but not phosphorylation of GSK3α and GSK3β, induced by PlGF (Fig. 7*B*). In contrast, the AKT inhibitor LY294002 suppressed PlGF-induced GSK3 phosphorylation in PlGF-knockdown hTERT-RPE1 cells (Fig. 7*C*). These results indicated that PlGF inactivated GSK3 *via* phosphorylation of AKT but not ERK1/2.
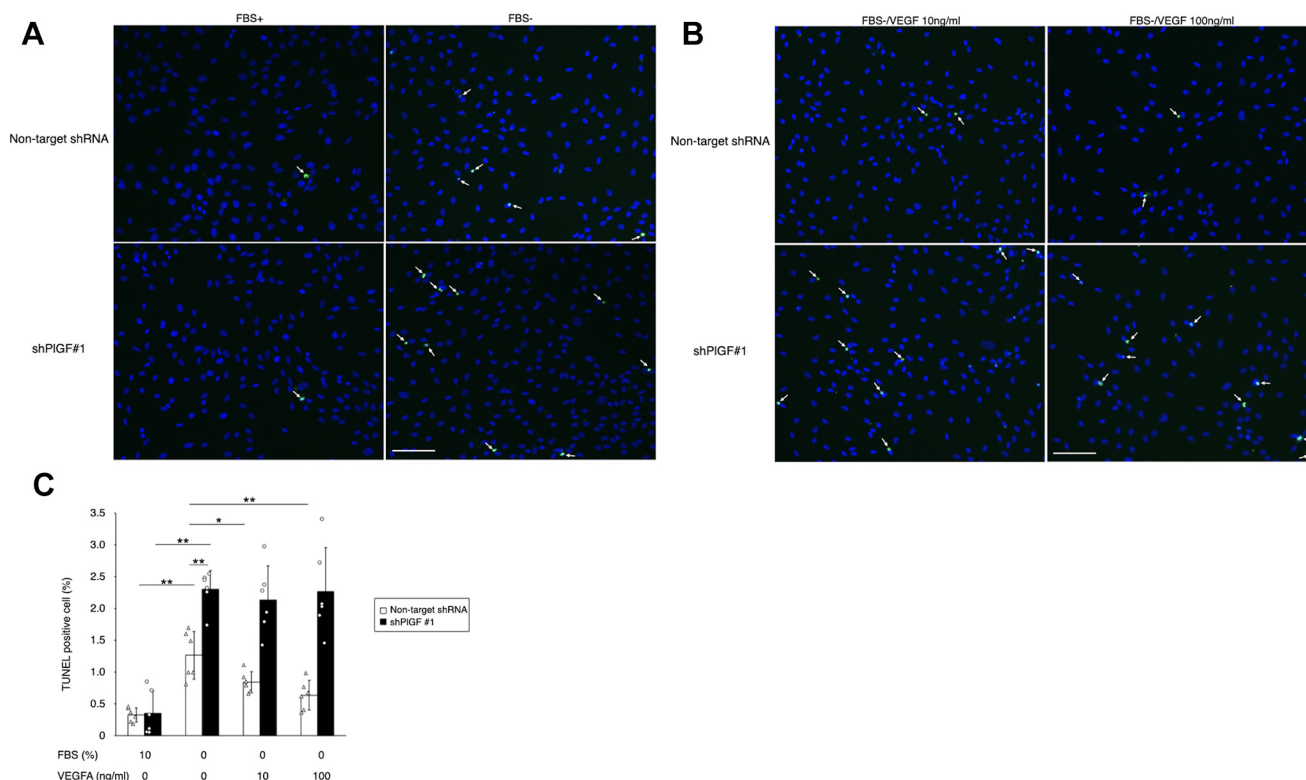
Figure 5. Impact of PlGF knockdown on the antiapoptotic effect of VEGFA in hTERT-RPE1. *A* and *B*, representative micrographs of TUNEL staining in nontarget shRNA and PlGF-knockdown hTERT-RPE1 clone #1. Cells were serum starved for 24 h with VEGFA recombinant protein (10–100 ng/ml). The scale bar represents 100 μm. *C*, TUNEL-positive cell rate of nontarget shRNA and PlGF-knockdown hTERT-RPE1 clone #1. Cells were serum starved for 24 h with VEGFA recombinant protein (10–100 ng/ml, n = 6 each, *$p < 0.05$, **$p < 0.01$). PlGF, placental growth factor; RPE, retinal pigment epithelium; VEGF, vascular endothelial growth factor A.

Discussion

In the present study, we demonstrated that (1) PlGF, similar to VEGFA, is a prerequisite for cell survival of RPE; (2) PlGF knockdown induces cell apoptosis and reduces the protein levels of VEGFR-2 in RPE; (3) PlGF protects VEGFR-2 protein from proteasomal degradation through GSK3 inactivation in RPE in an autocrine fashion; and (4) serine–threonine kinase AKT, but not ERK1/2, mediates GSK-3 inactivation. The current data indicate that PlGF contributes to the conservation of VEGFA/VEGFR-2 signaling *via* suppression of VEGFR-2 degradation through GSK3 inactivation, which is indispensable for the survival of RPE cells (Fig. 8).

In the eye, the retina consisting of the neural retina and RPE, a monolayer of pigmented cells, arises from the neuroectoderm (15). Despite their epithelial cellular characteristics, human RPE cells express the cognate receptors for VEGF family proteins, VEGFR-1 and VEGFR-2 (16). Furthermore, VEGFR-2 activation by VEGFA regulates the cellular functions of RPE, including its barrier properties (17) and its role in maintenance of cellular integrity (8). Therefore, lines of evidence suggest the pivotal role of the VEGFA/VEGF receptor axis in RPE homeostasis. In the present study, the number of apoptotic cells increased in hTERT-RPE1 cells exposed to serum starvation, which was substantially rescued by VEGFA. In addition, VEGFR-2 knockdown abolished the rescue effects of VEGFA in apoptotic hTERT-RPE1 cells. The current data indicate that VEGFR-2 mediates the protective effects of VEGFA in RPE cells under cellular stress.

Previous studies have also shown that human RPE cells secrete PlGF (14, 16). In addition, PlGF deficiency has been reported to lead to increased apoptosis and necrosis in vascular endothelial cells and macrophages (18). PlGF also acts as a survival factor in tumor cells (19) and in a variety of cell types (13, 20). In the current study, whereas PlGF-knockdown caused no alteration in the proliferation rate of hTERT-RPE1 cells, it enhanced serum starvation–induced apoptosis in RPE cells, which was reversed by replenishment of PlGF-1 and PlGF-2. In addition, PlGF knockdown enhanced the activation of caspases 3 and/or 7, both of which are executioner caspases carrying out the apoptosis cascade. Thus, the present study revealed that PlGF plays an antiapoptotic role against serum starvation–induced apoptosis in RPE cells. Since RPE is exposed to nutritional deficiency by hydrophobic changes in the Bruch's membrane of senile people with neovascular AMD, the antiapoptotic role of PlGF under serum starvation condition is most likely to be crucial when considering that macular atrophy increases after anti-VEGF treatment for neovascular AMD (9, 10). However, the current data contradict the findings of a previous study, in which suppression of the PlGF gene had no effect on RPE cell survival (21). This difference between the previous and current studies might be due to the methodology used for gene silencing, since the
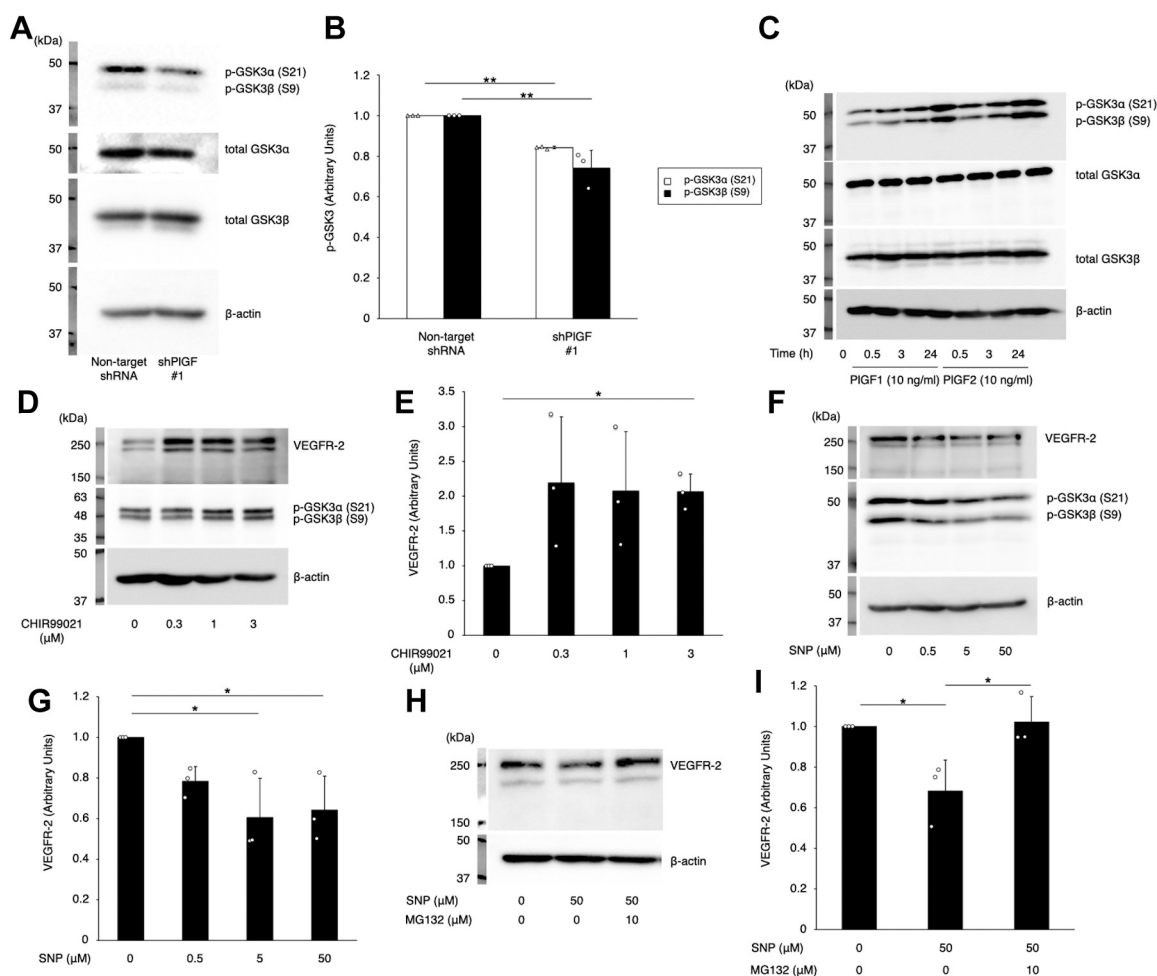
Figure 6. Role of GSK3 in proteasomal degradation of VEGFR-2 in PlGF-knockdown hTERT-RPE1. *A* and *B*, immunoblot for GSK3α, p-GSK3α, GSK3β, and p-GSK3β in nontarget shRNA and PlGF-knockdown hTERT-RPE1 clone #1 (n = 3 each, **$p < 0.01$). *C*, immunoblot for GSK3α, p-GSK3α, GSK3β, and p-GSK3β in PlGF-knockdown hTERT-RPE1 clone #1. Cells were serum starved for 17 h and treated with PlGF-1 or PlGF-2 recombinant protein (10 ng/ml) for the indicated time. *D* and *E*, immunoblot for VEGFR-2 and phosphorylation of GSK3α and GSK3β in PlGF-knockdown hTERT-RPE1 #1 treated with CHIR99021 for 2 h (0.3–3 μM, n = 3 each, *$p < 0.05$). *F* and *G*, immunoblot for VEGFR-2 and phosphorylation of GSK3α and GSK3β in hTERT-RPE1 treated with SNP for 1 h (0.5–50 μM, n = 3 each, *$p < 0.05$). *H* and *I*, immunoblot for VEGFR-2 in hTERT-RPE1 treated with SNP (50 μM) with or without MG132 (10 μM) for 1 h (n = 3 each, *$p < 0.05$). GSK3, glycogen synthase kinase 3; PlGF, placental growth factor; RPE, retinal pigment epithelium; VEGFR-2, vascular endothelial growth factor receptor-2.

previous study used transient RNA interference by siRNA and the present study used retrovirus vector–mediated stable gene silencing. Thus, our data suggest that long-term blockade of PlGF exacerbates RPE degeneration.

Notably, in the present study, we found that PlGF knockdown significantly reduced the protein level of VEGFR-2 in RPE cells, whereas the mRNA expression levels of *VEGFA*, *VEGFR1*, *VEGFR2*, *NRP1*, and *NRP2* did not change, indicating that PlGF is involved in the stabilization of the VEGFR-2 protein. Furthermore, the present data also demonstrated that the protective effect of VEGFA was abrogated by silencing of PlGF in hTERT-RPE1 cells. VEGFA signaling through VEGFR-2 is a major pathway that activates angiogenesis by inducing the proliferation, survival, and migration of endothelial cells (22). In addition to its protective effects in endothelial cells, VEGFA/VEGFR-2 signaling is also crucial for cytoprotective effects in a variety of neuronal tissues (23, 24). Taken together, the previous and present data suggest that PlGF is indispensable for cell survival of RPE by conserving

VEGFA signaling through VEGFR-2 protein stabilization. To date, several mechanisms have been proposed to explain the role of PlGF in the enhancement of VEGFA/VEGFR-2 signaling. For instance, PlGF has been suggested to displace VEGFA from VEGFR-1, thereby facilitating VEGFA binding to VEGFR-2 (25). Furthermore, the PlGF/VEGFA heterodimer has been proposed to enhance the formation of the VEGFR-1/VEGFR-2 heterodimer (6). In addition to the previous findings, the present data suggest a novel crosstalk mechanism between PlGF and the VEGFA/VEGFR-2 axis *via* VEGFR-2 protein stabilization. Thus, the present study might unexpectedly provide some insight into the crosstalk between VEGFR-1 and VEGFR-2. Further investigation is warranted to explore the mechanism underlying the association between VEGFR-1 and VEGFR-2.

GSK3, which consists of two structurally similar isoforms, GSK3α and GSK3β, is a proline-directed serine/threonine kinase originally identified as an enzyme involved in glycogen metabolism and subsequently shown to perform multiple
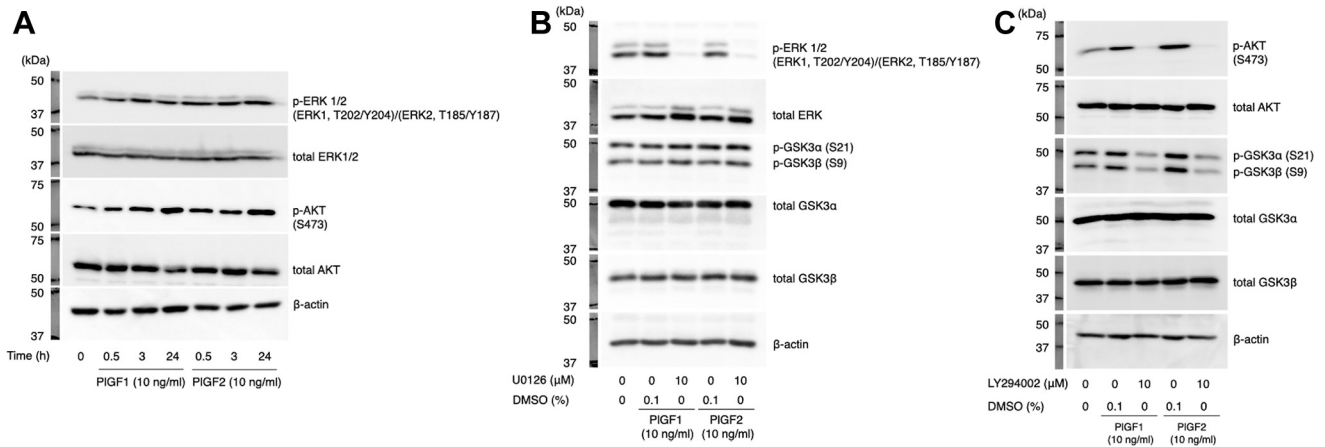
Figure 7. Roles of ERK1/2 and AKT in the PlGF-induced GSK3 phosphorylation in PlGF-knockdown hTERT-RPE1. *A,* immunoblot for ERK1/2 and AKT in nontarget shRNA and PlGF-knockdown hTERT-RPE1 clone #1 (n = 3 each, **$p < 0.01$). Cells were serum starved for 17 h and treated with PlGF-1 or PlGF-2 recombinant protein (10 ng/ml) for the indicated time. *B,* immunoblot for ERK1/2, p-ERK1/2, GSK3α, p-GSK3α, GSK3β, and p-GSK3β in PlGF-knockdown hTERT-RPE1 clone #1. Cells were serum starved for 17 h and treated with PlGF-1 or PlGF-2 recombinant protein (10 ng/ml) with or without U0126 (10 μM) or 0.1% DMSO as a solvent control for 3 h. *C,* immunoblot for AKT, p-AKT, GSK3α, p-GSK3α, GSK3β, and p-GSK3β in PlGF-knockdown hTERT-RPE1 clone #1. Cells were serum starved for 17 h and treated with PlGF-1 or PlGF-2 recombinant protein (10 ng/ml) with or without LY294002 (10 μM) or 0.1% DMSO for 3 h. DMSO, dimethyl sulfoxide; ERK1/2, extracellular signal–regulated kinase 1/2; GSK3, glycogen synthase kinase 3; PlGF, placental growth factor; RPE, retinal pigment epithelium.

molecular functions in important biological processes ([26], [27]). In addition, GSK3 regulates the ubiquitination and proteasomal degradation of several proteins, including glycogen synthase and β-catenin ([28]). More recently, GSK3 was shown to enhance proteasomal degradation of VEGFR-2 by regulating the binding of β-transducin repeats containing E3 ubiquitin protein ligase to VEGFR-2 ([29]), and GSK3 activity is inhibited by AKT that phosphorylates the serine residues Ser21 in GSK3α and Ser9 in GSK3β ([30]). In this study, we demonstrated that PlGF suppresses the proteasomal degradation of VEGFR2 through GSK3 inactivation *via* phosphorylation of AKT but not ERK1/2. As previously reported, PlGF binds to VEGFR-1 and phosphorylates AKT in tumor cells, which in turn increases cell viability ([19]). Furthermore, it has been elucidated that multiple signaling pathways, including Akt, protein kinase A, protein kinase C, and other kinases, increase the serine phosphorylation of GSK3, resulting in the inhibition

of GSK3 activity ([30]). Therefore, the current data indicate that AKT phosphorylation is one of the signaling pathway downstream of the PlGF–VEGFR-1 axis, resulting in GSK3 inactivation and VEGFR-2 stabilization in RPE. Further studies are needed to elucidate the signaling pathways to inactivate GSK3 in RPE exposed to PlGF.

The limitations of this study are as follows. First, the effect of PlGF on VEGFR-2 was relatively partial, and the apoptotic cells after the knockdown of VEGFR-2 were fewer than PlGF knockdown, indicating the presence of other mechanisms to protect the RPE against PlGF blockade. Second, in the present study, we did not check whether the cytoprotective effect of PlGF was mediated only by VEGFR-1 or *via* NRP-1 and/or NRP-2. Third, in this study, all experiments were conducted using the immortalized RPE cell line hTERT-RPE1 alone. Whereas we sought to reproduce the experimental outcomes of this study using human-induced pluripotent stem cell–derived RPE, the *VEGFR2* mRNA expression was not significantly decreased in the PlGF knockdown induced pluripotent stem cell–derived RPE by transient transfection using siRNA strategy (data not shown). It was previously demonstrated that basal VEGFR-2 levels were different between the astrocytes captured from frontal cortex and those from parietal–occipital cortex in PlGF$^{-/-}$ mice, presumably caused by the heterogeneity of the astroglial cell populations present in different brain regions ([31]). The previous and current studies might indicate that the responses against PlGF stimulation are dependent on the cell types and conditions. Further investigations are required to clarify these questions.

In summary, our data showed that PlGF is important for RPE cell viability and that PlGF supports VEGFA/VEGFR-2 signaling by stabilizing VEGFR-2 protein through GSK3 inactivation. The deleterious influence of long-term blockade of VEGF family proteins in patients with neovascular AMD has
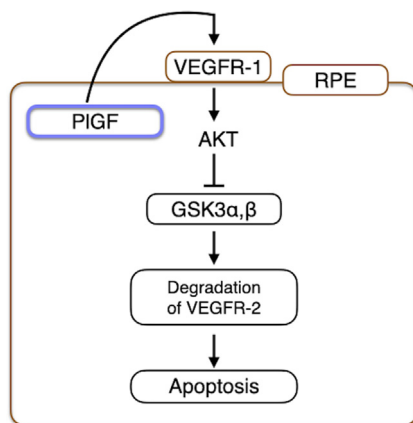

Figure 8. A schematic figure depicting the proposed mechanism of VEGFR-2 stabilization and the antiapoptotic effect of PlGF in RPE. PlGF, placental growth factor; RPE, retinal pigment epithelium; VEGFR-2, vascular endothelial growth factor receptor 2.

been discussed, and it remains a topic of debate. The present study provides novel information about the physiological role of PlGF in the RPE and presents the possibility that long-term blockade of PlGF also accelerates macular atrophy in patients with neovascular AMD receiving continuous anti-VEGF agents targeting PlGF and VEGFA.

Experimental procedures

Cell culture

The human RPE cell line hTERT-RPE1 (American Type Culture Collection) was cultured at 37 °C in Dulbecco's modified Eagle's medium (DMEM)/F-12 (Fuji Film Wako Pure Chemicals) supplemented with 10% fetal bovine serum (Thermo Fisher Scientific) in a temperature-controlled 37 °C incubator with an atmosphere of 95% air and 5% CO_2.

RNA interference by retrovirus-based shRNA

The shRNA constructs for human PlGF (pMLP-PGF-sh1, clone ID: RLGH-GU47797) and nontarget control shRNA were purchased from TransOMIC. Retroviral constructs were transfected into Phoenix-Ampho packaging cells (American Type Culture Collection) using X-tremeGene HP DNA transfection reagent (Merck). After 24 h of incubation, the culture media were harvested and centrifuged at $300g$ for 5 min. For retroviral transduction, hTERT-RPE1 (2×10^5 cells) were seeded with DMEM/F-12 in 6-well plates, and fresh DMEM/F-12 (1 ml) and virus-containing supernatant supplemented with 5 μg/ml polybrene (1 ml) were added to the culture wells after washing out of the culture media after 24 h of incubation. Subsequently, the plate was centrifuged at $1000g$ for 60 min at room temperature. Drug selection and cell cloning were conducted in the presence of 12 μg/ml puromycin using the limited dilution method.

Quantitative real-time PCR

Total RNA was extracted from hTERT-RPE1 cells using TRI reagent (Molecular Research Center) and reverse transcribed to complementary DNA (cDNA) using GoScript reverse transcriptase (Promega). Real-time PCR was performed using GoTaq qPCR Master Mix (Promega) in a StepOnePlus Real-Time PCR System (Thermo Fisher Scientific). The primer sequences used for real-time PCR and the expected size of the amplification products were as follows: 5′-AACGGCTCGTCAGAGGTG-3′ (forward) and 5′-AGACACAGGATGGGCTGAAC-3′ (reverse) for human *PlGF* (NM_002632.6), 139 bp; 5′-AGGGCAGAATCATCACGAAG-3′ (forward) and 5′-CACACAGGATGGCTTGAAGA-3′ (reverse) for human *VEGFA* (NM_001171626.1), 136 bp; 5′-ACCACTCCCTTGAACACGAG-3′ (forward) and 5′-TGCTTTGGTCAATTCGTCGC-3′ (reverse) for human *VEGFR1* (NM_002019.4), 94 bp; 5′-AGACCGGCTGAAGC-TAGGTA-3′ (forward) and 5′-CGATGCTCACTGTGTGTTGC-3′ (reverse) for human *VEGFR2* (NM_002253.3), 147 bp; 5′-CGAGCACAGAGCCTCGCCTT-3′ (forward) and 5′-AGCGCGGCGATATCATCATCC-3′ (reverse) for human *ACTB* (NM_001101.5), 83 bp. The PCR conditions used in the current study were as follows: 95 °C for 2 min, followed by 95 °C for 15 s, and 60 °C for 1 min for 40 cycles. All data were calculated using the ΔΔCt method, with the level of *ACTB* mRNA as the normalization control.

ELISA for the cell culture supernatants

hTERT-RPE1 and shRNA-transfected cell clones were seeded into a 10-cm dish at a density of 1.2×10^6 cells and incubated for 24 h. The cells were serum starved and cultured for 48 h. The supernatants were collected and centrifuged at $1000g$ for 10 min at 4 °C. Protein levels of PlGF and VEGFA in the supernatants were measured using a sandwich ELISA kit (R&D Systems) after normalization to the total protein levels measured using a bicinchoninic acid protein assay kit (Thermo Fisher Scientific).

RT–PCR

Total RNA was extracted from hTERT-RPE1 and PlGF-knockdown hTERT-RPE1 cells and reverse transcribed to cDNA using GoScript reverse transcriptase. RT–PCR was performed using Ex Taq hot start version (Takara Bio, Inc) on the Mastercycler nexus (Eppendorf). The primer sequences and the expected size of the amplification products were as follows: 5′-CTCCTAAAGATCCGTTCTGG-3′ (forward) and 5′-ATAAATACACGAGCCGGGTG-3′ (reverse) for human *PlGF-1*: 182 bp, *PlGF-2*: 245 bp, *PlGF-3*: 398 bp, and *PlGF-4*: 462 bp. PCR conditions used were 95 °C for 2 min; followed by 95 °C for 30 s, 55 °C for 30 s, and 72 °C for 30 s for 35 cycles; and 72 °C for 5 min. Water was used instead of cDNA as a nontemplate control. The products were electrophoresed in 2.5% agarose gels, stained with SYBR Safe (Thermo Fisher Scientific), and visualized under UV irradiation.

Cell proliferation assay

Cell proliferation assays were performed using the Cell Counting Kit-8 (Dojindo). hTERT-RPE1 and shRNA-transfected cell clones were seeded into four 96-well plates at a density of 5×10^3 cells/well and incubated at 37 °C in a humidified atmosphere (95% air, 5% CO_2). Immediately after cell seeding (time 0) or after 24 to 72 h of incubation, CCK8 solution (10 μl) was added to each well of the plate. Cells were incubated for 1.5 h at 37 °C in a humidified atmosphere, and the absorbance was measured at 450 nm by using a microplate reader.

TUNEL

hTERT-RPE1 and shRNA-transfected cell clones were seeded into 4-well slide chambers at a density of 7.5×10^4 cells/well and incubated for 24 h. Cells were serum starved with or without recombinant human proteins of PlGF-1 (0.1–10 ng/ml), PlGF-2 (0.1–10 ng/ml), and VEGFA (10–100 ng/ml; R&D Systems) for 24 h. The TUNEL assay was performed using ApopTag Fluorescein Direct *In Situ* Apoptosis Detection Kit (Merck).

Caspase 3/7 activity assay

hTERT-RPE1 and shRNA-transfected cell clones were seeded into individual wells of a clear bottom 96-well plate at a density of 1.4×10^4 cells/well and incubated for 24 h. Cells were serum starved for 24 h. Caspase 3/7 activity was measured by Caspase-Glo 3/7 assay (Promega).

RNA interference by VEGFR2 siRNA

siRNA oligonucleotides for suppression of *VEGFR2* gene expression (siRNA-1, silencer select siRNA ID: s7822; siRNA-2, silencer select siRNA ID: s7823) and a negative control siRNA oligo (silencer select negative control no. 1) were purchased from Thermo Fisher Scientific and used at a concentration of 10 nM. Cells were transfected with siRNA using Lipofectamine RNAiMAX reagent (Thermo Fisher Scientific).

Western blotting

Cells were lysed in 1× Laemmli buffer (62.5 mM Tris–HCl [pH 6.8], 2% SDS, 10% glycerol, 0.01% bromophenol blue, and 5% 2-mercaptoethanol). The cell lysates were sonicated three times for 5 s each on ice and centrifuged at $15,000g$ for 10 min at 4 °C. Protein concentrations of the samples were measured using a bicinchoninic acid protein assay kit and adjusted to 2 mg/ml. The samples were boiled at 95 °C for 3 min, separated by SDS-polyacrylamide gel electrophoresis, and electroblotted onto polyvinylidene fluoride membranes (Merck). The membranes were blocked with 5% skim milk, incubated with primary antibody at 4 °C overnight, and then incubated with goat anti-rabbit immunoglobulin G (H + L) horseradish peroxidase conjugate (1:4000 dilution; Promega) or goat antimouse immunoglobulin G (H + L) horseradish peroxidase conjugate (1:4000 dilution; Jackson Immuno Research Laboratories, Inc) at room temperature for 1 h. The primary antibodies used for Western blotting were as follows: phospho-GSK3α/β (1:1000 dilution, catalog no.: D17D2, rabbit monoclonal), GSK3α (1:1000 dilution, catalog no.: D80E6, rabbit monoclonal), GSK3β (1:1000 dilution, catalog no.: D5C5Z, rabbit monoclonal), VEGFR-2 (1:1000 dilution, catalog no.: D5B1, rabbit monoclonal), phospho-ERK1/2 (1:1000 dilution, catalog no.: D13.14.4E, rabbit monoclonal), ERK1/2 (1:1000 dilution, catalog no.: L34F12, mouse monoclonal), phospho-AKT (1:1000 dilution, catalog no.: D9E, rabbit monoclonal), and AKT (1:1000 dilution, catalog no.: 9272, rabbit polyclonal). All antibodies were purchased from Cell Signaling Technology. Signals were visualized using SuperSignal West Pico Chemiluminescent Substrate (Thermo Fisher Scientific). β-Actin antibody (1:1000 dilution, catalog no.: PM053; rabbit polyclonal) was purchased from MBL Life Science.

Statistical analysis

All results are presented as the mean ± SD. Student's *t* test was used for pairwise statistical comparisons between groups, and one-way ANOVA, followed by the post hoc Tukey–Kramer test, if appropriate, was used for multiple comparisons. Differences in the means were considered statistically significant at $p < 0.05$.

Data availability

All data are contained within the article.

Abbreviations—The abbreviations used are: AMD, age-related macular degeneration; cDNA, complementary DNA; DMEM, Dulbecco's modified Eagle's medium; ERK, extracellular signal–regulated kinase; NRP, neuropilin; PlGF, placental growth factor; RPE, retinal pigment epithelium; VEGF, vascular endothelial growth factor; VEGFR-2, VEGF receptor-2.

References

1. Ribatti, D. (2008) The discovery of the placental growth factor and its role in angiogenesis: a historical review. *Angiogenesis* **11**, 215–221
2. Odorisio, T., Schietroma, C., Zaccaria, M. L., Cianfarani, F., Tiveron, C., Tatangelo, L., *et al.* (2002) Mice overexpressing placenta growth factor exhibit increased vascularization and vessel permeability. *J. Cell Sci.* **115**, 2559–2567
3. Oura, H., Bertoncini, J., Velasco, P., Brown, L. F., Carmeliet, P., and Detmar, M. (2003) A critical role of placental growth factor in the induction of inflammation and edema formation. *Blood* **101**, 560–567
4. Yang, W., Ahn, H., Hinrichs, M., Torry, R. J., and Torry, D. S. (2003) Evidence of a novel isoform of placenta growth factor (PlGF-4) expressed in human trophoblast and endothelial cells. *J. Reprod. Immunol.* **60**, 53–60
5. Van Bergen, T., Etienne, I., Cunningham, F., Moons, L., Schlingemann, R. O., Feyen, J. H. M., *et al.* (2019) The role of placental growth factor (PlGF) and its receptor system in retinal vascular diseases. *Prog. Retin. Eye Res.* **69**, 116–136
6. Autiero, M., Waltenberger, J., Communi, D., Kranz, A., Moons, L., Lambrechts, D., *et al.* (2003) Role of PlGF in the intra- and intermolecular cross talk between the VEGF receptors Flt1 and Flk1. *Nat. Med.* **9**, 936–943
7. Byeon, S. H., Lee, S. C., Choi, S. H., Lee, H. K., Lee, J. H., Chu, Y. K., *et al.* (2010) Vascular endothelial growth factor as an autocrine survival factor for retinal pigment epithelial cells under oxidative stress *via* the VEGF-R2/PI3K/Akt. *Invest. Ophthalmol. Vis. Sci.* **51**, 1190–1197
8. Ford, K. M., Saint-Geniez, M., Walshe, T., Zahr, A., and D'Amore, P. A. (2011) Expression and role of VEGF in the adult retinal pigment epithelium. *Invest. Ophthalmol. Vis. Sci.* **52**, 9478–9487
9. Hata, M., Oishi, A., Tsujikawa, A., Yamashiro, K., Miyake, M., Ooto, S., *et al.* (2014) Efficacy of intravitreal injection of aflibercept in neovascular age-related macular degeneration with or without choroidal vascular hyperpermeability. *Invest. Ophthalmol. Vis. Sci.* **55**, 7874–7880
10. Kuroda, Y., Yamashiro, K., Tsujikawa, A., Ooto, S., Tamura, H., Oishi, A., *et al.* (2016) Retinal pigment epithelial atrophy in neovascular age-related

macular degeneration after ranibizumab treatment. *Am. J. Ophthalmol.* **161**, 94–103.e101

11. Rofagha, S., Bhisitkul, R. B., Boyer, D. S., Sadda, S. R., Zhang, K., and Group, S.-U. S. (2013) Seven-year outcomes in ranibizumab-treated patients in ANCHOR, MARINA, and HORIZON: a multicenter cohort study (SEVEN-UP). *Ophthalmology* **120**, 2292–2299

12. Nishijima, K., Ng, Y. S., Zhong, L., Bradley, J., Schubert, W., Jo, N., *et al.* (2007) Vascular endothelial growth factor-A is a survival factor for retinal neurons and a critical neuroprotectant during the adaptive response to ischemic injury. *Am. J. Pathol.* **171**, 53–67

13. Cai, J., Ahmad, S., Jiang, W. G., Huang, J., Kontos, C. D., Boulton, M., *et al.* (2003) Activation of vascular endothelial growth factor receptor-1 sustains angiogenesis and Bcl-2 expression *via* the phosphatidylinositol 3-kinase pathway in endothelial cells. *Diabetes* **52**, 2959–2968

14. Miyamoto, N., de Kozak, Y., Jeanny, J. C., Glotin, A., Mascarelli, F., Massin, P., *et al.* (2007) Placental growth factor-1 and epithelial haemato-retinal barrier breakdown: potential implication in the pathogenesis of diabetic retinopathy. *Diabetologia* **50**, 461–470

15. Bharti, K., Miller, S. S., and Arnheiter, H. (2011) The new paradigm: retinal pigment epithelium cells generated from embryonic or induced pluripotent stem cells. *Pigment Cell Melanoma Res.* **24**, 21–34

16. Hollborn, M., Tenckhoff, S., Seifert, M., Kohler, S., Wiedemann, P., Bringmann, A., *et al.* (2006) Human retinal epithelium produces and responds to placenta growth factor. *Graefes Arch. Clin. Exp. Ophthalmol.* **244**, 732–741

17. Ablonczy, Z., and Crosson, C. E. (2007) VEGF modulation of retinal pigment epithelium resistance. *Exp. Eye Res.* **85**, 762–771

18. Adini, A., Kornaga, T., Firoozbakht, F., and Benjamin, L. E. (2002) Placental growth factor is a survival factor for tumor endothelial cells and macrophages. *Cancer Res.* **62**, 2749–2752

19. Albonici, L., Doldo, E., Palumbo, C., Orlandi, A., Bei, R., Pompeo, E., *et al.* (2009) Placenta growth factor is a survival factor for human malignant mesothelioma cells. *Int. J. Immunopathol Pharmacol.* **22**, 389–401

20. Akrami, H., Mehdizadeh, K., Moradi, B., Borzabadi Farahani, D., Mansouri, K., and Ghalib Ibraheem Alnajar, S. (2019) PlGF knockdown induced apoptosis through Wnt signaling pathway in gastric cancer stem cells. *J. Cell Biochem.* **120**, 3268–3276

21. Akrami, H., Soheili, Z. S., Sadeghizadeh, M., Ahmadieh, H., Rezaeikanavi, M., Samiei, S., *et al.* (2011) PlGF gene knockdown in human retinal pigment epithelial cells. *Graefes Arch. Clin. Exp. Ophthalmol.* **249**, 537–546

22. Shibuya, M., and Claesson-Welsh, L. (2006) Signal transduction by VEGF receptors in regulation of angiogenesis and lymphangiogenesis. *Exp. Cell Res.* **312**, 549–560

23. Foxton, R. H., Finkelstein, A., Vijay, S., Dahlmann-Noor, A., Khaw, P. T., Morgan, J. E., *et al.* (2013) VEGF-A is necessary and sufficient for retinal neuroprotection in models of experimental glaucoma. *Am. J. Pathol.* **182**, 1379–1390

24. Jin, K. L., Mao, X. O., and Greenberg, D. A. (2000) Vascular endothelial growth factor: direct neuroprotective effect in *in vitro* ischemia. *Proc. Natl. Acad. Sci. U. S. A.* **97**, 10242–10247

25. Cao, Y. (2009) Positive and negative modulation of angiogenesis by VEGFR1 ligands. *Sci. Signal.* **2**, re1

26. McCubrey, J. A., Rakus, D., Gizak, A., Steelman, L. S., Abrams, S. L., Lertpiriyapong, K., *et al.* (2016) Effects of mutations in Wnt/beta-catenin, hedgehog, Notch and PI3K pathways on GSK-3 activity-diverse effects on cell growth, metabolism and cancer. *Biochim. Biophys. Acta* **1863**, 2942–2976

27. Plyte, S. E., Hughes, K., Nikolakaki, E., Pulverer, B. J., and Woodgett, J. R. (1992) Glycogen synthase kinase-3: functions in oncogenesis and development. *Biochim. Biophys. Acta* **1114**, 147–162

28. Cohen, P., and Frame, S. (2001) The renaissance of GSK3. *Nat. Rev. Mol. Cell Biol.* **2**, 769–776

29. Wu, W., Zhang, D., Pan, D., Zuo, G., Ren, X., and Chen, S. (2016) Downregulation of vascular endothelial growth factor receptor-2 under oxidative stress conditions is mediated by beta-transduction repeat-containing protein *via* glycogen synthase kinase-3beta signaling. *Int. J. Mol. Med.* **37**, 911–920

30. Beurel, E., Grieco, S. F., and Jope, R. S. (2015) Glycogen synthase kinase-3 (GSK3): regulation, actions, and diseases. *Pharmacol. Ther.* **148**, 114–131

31. Freitas-Andrade, M., Carmeliet, P., Stanimirovic, D. B., and Moreno, M. (2008) VEGFR-2-mediated increased proliferation and survival in response to oxygen and glucose deprivation in PlGF knockout astrocytes. *J. Neurochem.* **107**, 756–767